M. Koskenvuori and I. Tittonen, GHz-range FSK-reception with microelectromechanical resonators, Sensors and Actuators A: Physical, 142, pp. 346-351 (2008).

GHz-range FSK-reception with microelectromechanical resonators

M. Koskenvuori [a,b,*], I. Tittonen [a,b]

[a] *Micro- and nanosciences, P.O. Box 3500, FIN-02015 TKK, Finland*
[b] *Center for New Materials, TKK, Finland*

Abstract

A micromechanical resonator with eigenfrequencies in the MHz-region is excited by using an AM-modulated GHz-range signal. The excitation voltage is down-converted to a force at the fundamental frequency of the resonator by voltage-force-non-linearity of the electromechanical transducer. Measurements are verified by simulations with excellent agreement. Finally, a method of coding information bits is presented and tested.
© 2007 Elsevier B.V. All rights reserved.

Keywords: MEMS; Resonator; Non-linearity; FSK

1. Introduction

Ever since the introduction of IC-compatible mechanical resonator for filtering applications [1] resonating MEMS devices have been promising an increasing level of integration in wireless communication systems. To fulfil this promise MEMS devices for various tasks have been implemented and presented. These include at least oscillators, filters and switches. Besides being ideal for filtering and oscillator applications due to the high Q-factor, MEMS-devices have been utilised for direct conversion architecture [2] and several MEMS-solutions combining mixing and filtering have been presented [3–5]. In a different kind of approach a capacitive MEMS-resonator operating at GHz-range has been used in channel selection for MEMS-based transceiver [6].

Direct conversion approach requires a local oscillator (LO) signal to be available at reception. Although this local oscillator signal can be used to amplify the reception, in very low power consumption applications it may be inconvenient. Another approach is to use specific input signals that are intrinsically converted from the high communication frequency down to the eigenfrequency of the MEMS-device through non-linear processes.

In this work we use a submicron-gap micromechanical resonator that is actuated by AM-modulated GHz-range signal

$$U(t) = U_0(1 + m\cos(2\pi f_m t))\cos(2\pi f_c t)$$
$$= U_0[\cos(2\pi f_c t) + m/2\cos 2\pi(f_c \pm f_m)t], \quad (1)$$

where m is the modulation index (≤ 1), f_c the carrier frequency and f_m the modulation frequency, which is also the resonance frequency f_r of the resonator. The modulation index m is the ratio of the carrier signal and the modulator signal amplitudes and defined to be $m \leq 1$. Spectrum of the signal with $m = 1$ is shown in Fig. 1.

The down-conversion of the signal is done with the capacitive coupling gap, where the actuating force F is related to the applied voltage U by $F = (1/2)U^2(\partial C/\partial x)$. This non-linear relation ensures that the arising force F has a component also at the resonator's resonance frequency $f_r = f_m$:

$$F_{f_m} = \left(\frac{1}{4}U_0^2 m + \frac{1}{4}U_0^2 m\right)\frac{\partial C}{\partial x} = \frac{1}{2}U_0^2 m\frac{\partial C}{\partial x}, \quad (2)$$

where $\partial C/\partial x$ is the electro-mechanical coupling factor. From Eq. (2) it is clear that the excitation force is at maximum with the modulation index $m = 1$ or when the amplitudes of the carrier and the sidebands are equal.

---

* Corresponding author. Tel.: +358 9 451 2948; fax: +358 9 451 3128.
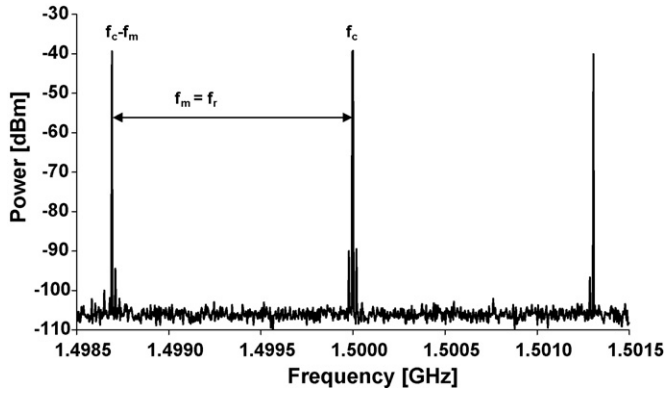*E-mail address:* mika.koskenvuori@tkk.fi (M. Koskenvuori).

Fig. 1. Spectrum of the input signal. The spectral components are selected so that the distance of the sidebands from the carrier coincides with the eigenfrequency f_r of the resonator. With non-linear voltage-force relation of the transducer gap this gives a rise to a force at the frequency $f_c - f_m = f_r$.

2. Device and simulation

The resonator used is an improved version of an earlier double-ended tuning-fork (DETF)-resonator (Fig. 2) used in [4]. The improvement is the reduction of the coupling gap d from $d = 1\,\mu m$ to $d \approx 170\,nm$ with polysilicon deposition [7]. The resonator was fabricated at VTT Technical Research Centre of Finland.

Before the down-conversion measurements, transmission (S_{21}) responses of the resonator with varying bias (U_{DC}) levels were recorded (Fig. 3). This was done to characterise the relevant physical and electrical parameters of the resonator in order to generate an accurate model of the resonator for a circuit simulator [8] (Fig. 4). The resonator was modelled as an electrical equivalent of the spring-mass system and for the capacitive coupling a model taking into account the usual second order force-voltage and also the third order capacitive non-linearity was used [9]. Initially the simulations were based on the use of transient model, but they were refined by using large-signal harmonic balance (HB) analysis utilising multiple independent
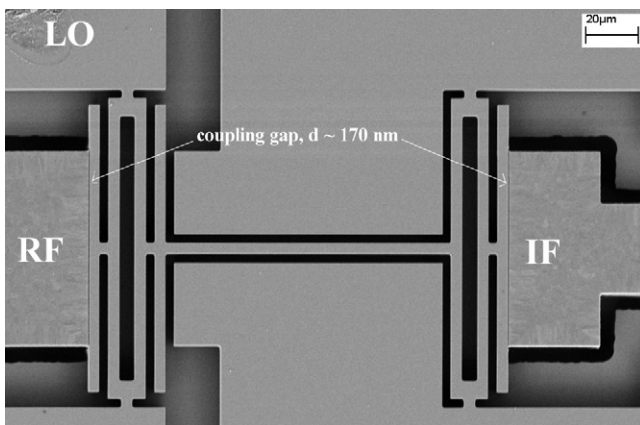

Fig. 2. A SEM-view of the used DETF-resonator. The resonator is fabricated on an SOI–wafer with DRIE. The coupling gap width of the electromechanical transducer is $d \approx 170\,nm$. The labels [RF, LO, IF] correspond to the labels of the electrodes used throughout the text.
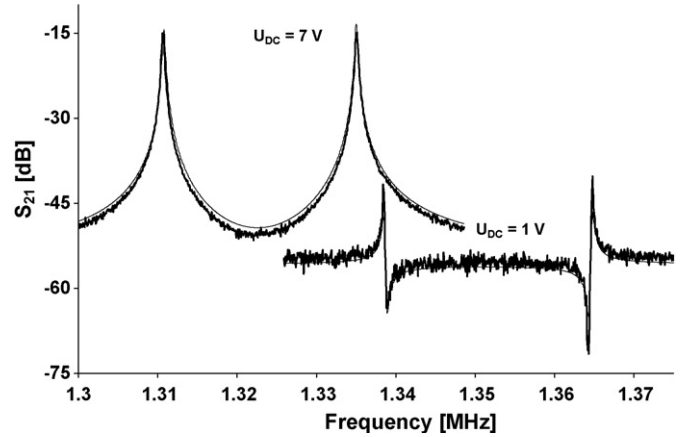

Fig. 3. Measured transmission (solid black line) and phase (dotted grey line) responses of the resonator used. Here, $U_{dc} = [1,\ 7]\,V$ and $P_{ac} = -45\,dBm$.

input and output tones (excitation frequencies) and their harmonics. Especially, for devices with high quality factors and therefore long settling times, HB analysis (carried out in frequency domain) is very efficient when compared to transient analysis (carried out in time domain) [10].

3. Measurements

3.1. Down-conversion

In order to study the excitation of the resonator using a GHz-range signal, the AM-modulated signal was coupled to the resonator via the RF-electrode and the signal at frequency $f_m = f_r$ was recorded from the IF-electrode with the aid of a DC-bias voltage $U_{DC} = 7\,V$. The resonator was grounded via the LO-electrode. The schematic of the measurement set-up is given in Fig. 5. Fig. 6 shows the down-converted signal strength as the modulation signal at the frequency f_m is swept over the two resonances with carrier signal at frequency $f_c = 1.5\,GHz$. The input signal power is $P_c = P_m = -33.5\,dBm$.

As suggested by Eq. (2), the down-conversion process should be relative to the second power of the input signal strength due to the effective multiplication of the spectral components at the carrier frequency and the sidebands. Fig. 7 shows the measured and simulated output signal voltage (V_{out}) of the resonator actuated with a modulated GHz-range signal (V_{in}, $f_c = [0.5,\ 1.5]\,GHz$) (Eq. (1)). It is evident that Figs. 6 and 7 both indicate a successful excitation of a MHz-range resonator ($f_r = f_m = 1.335\,MHz$) with a GHz-range signal.

When the carrier signal frequency f_c is increased further the conversion efficiency of the device can be seen to degrade. This behaviour is visible for in Fig. 8. From simulated results the speed of degradation can be calculated to be $-8.3\,dB/GHz$, which is in agreement with the measurements.

3.2. Signal reception

The two resonances of the device give an opportunity to utilise the resonator as a frequency shift keying (FSK)-receiver where the information is coded into the two frequency components
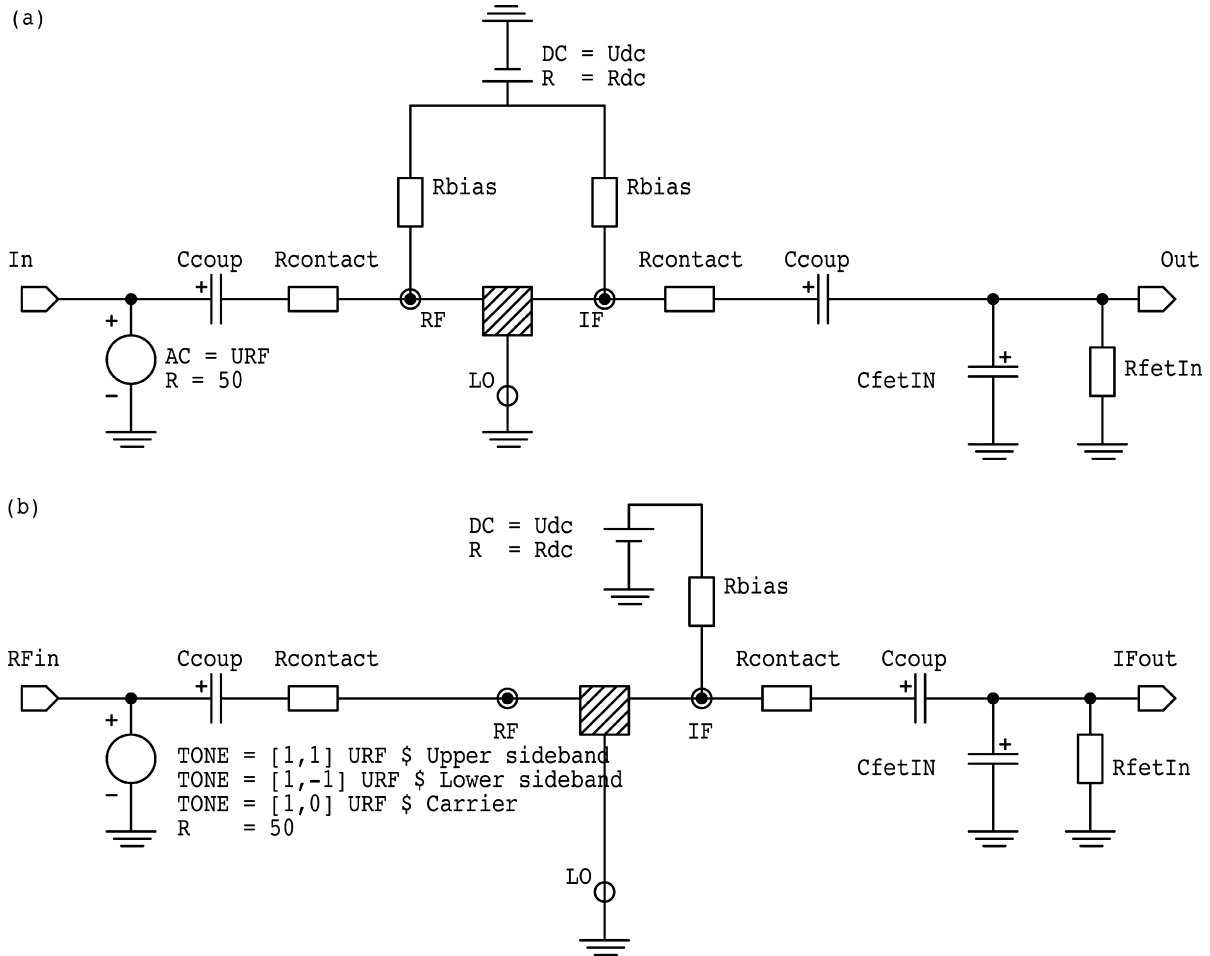
Fig. 4. (a) The simulation and measurement set-up used for the transmission measurements. (b) The set-up used for down-conversion simulations. The resonator is modelled inside the three terminal black-box containing e.g. spring-mass model of the resonator, electromechanical transducers and the parasitic capacitances. The preamplifier is modelled as the input capacitance and resistance of the FET at the input of the first stage of the amplifier.
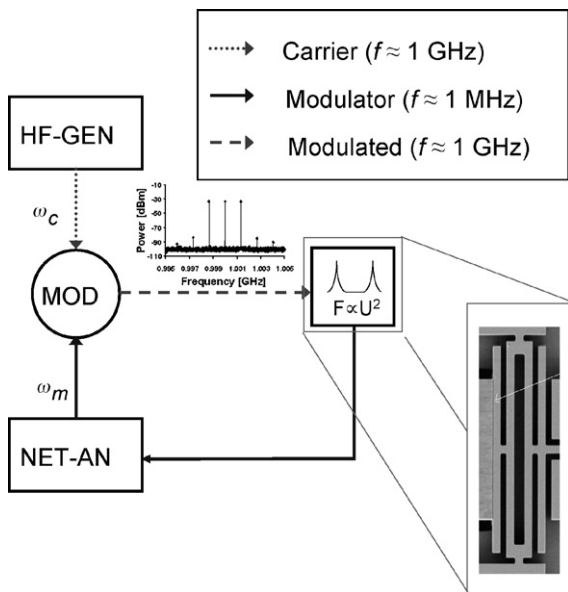

Fig. 5. Measurement scheme for the down-conversion measurements. AM-modulated signal was coupled to RF-electrode and the demodulated resonance signal was measured from the DC-biased IF-electrode. The resonator was grounded via the LO-electrode.
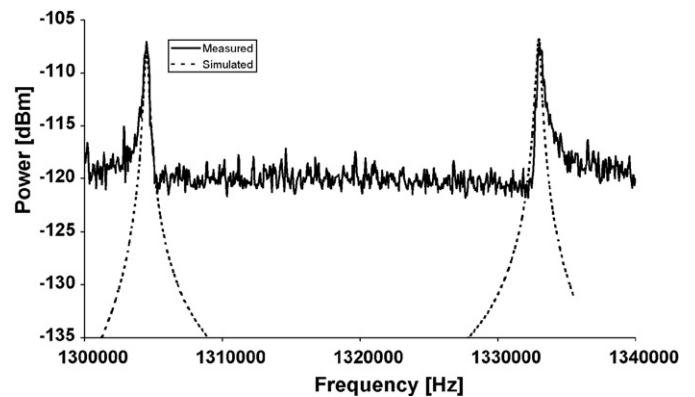

Fig. 6. Modulation signal at frequency f_m is swept over both resonances, while carrier signal frequency is constant $f_c = 1.5\,\text{GHz}$. The region between the resonances falls below the noise level of the measurement set-up, but the match between the measurement and simulation at the resonances is satisfactory.
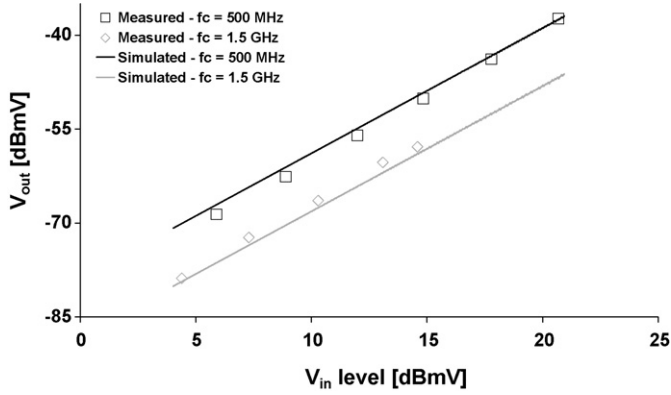
Fig. 7. Output signal voltage V_{out} as a function of input signal voltage V_{in}. The figure indicates a successful excitation of MHz-range resonator with GHz-range signal as the carrier frequency of the excitation signal is $f_{in} = [0.5, 1.5]$ GHz and the recorded output signal frequency $f_{out} = f_m = 1.335$ MHz.
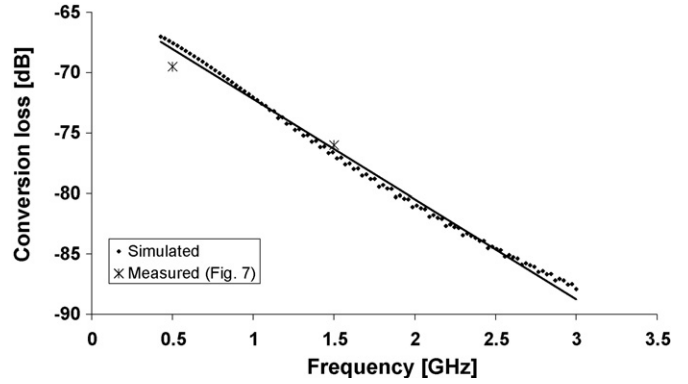
Fig. 8. Conversion efficiency of the demodulator as a function of the carrier signal frequency f_c.
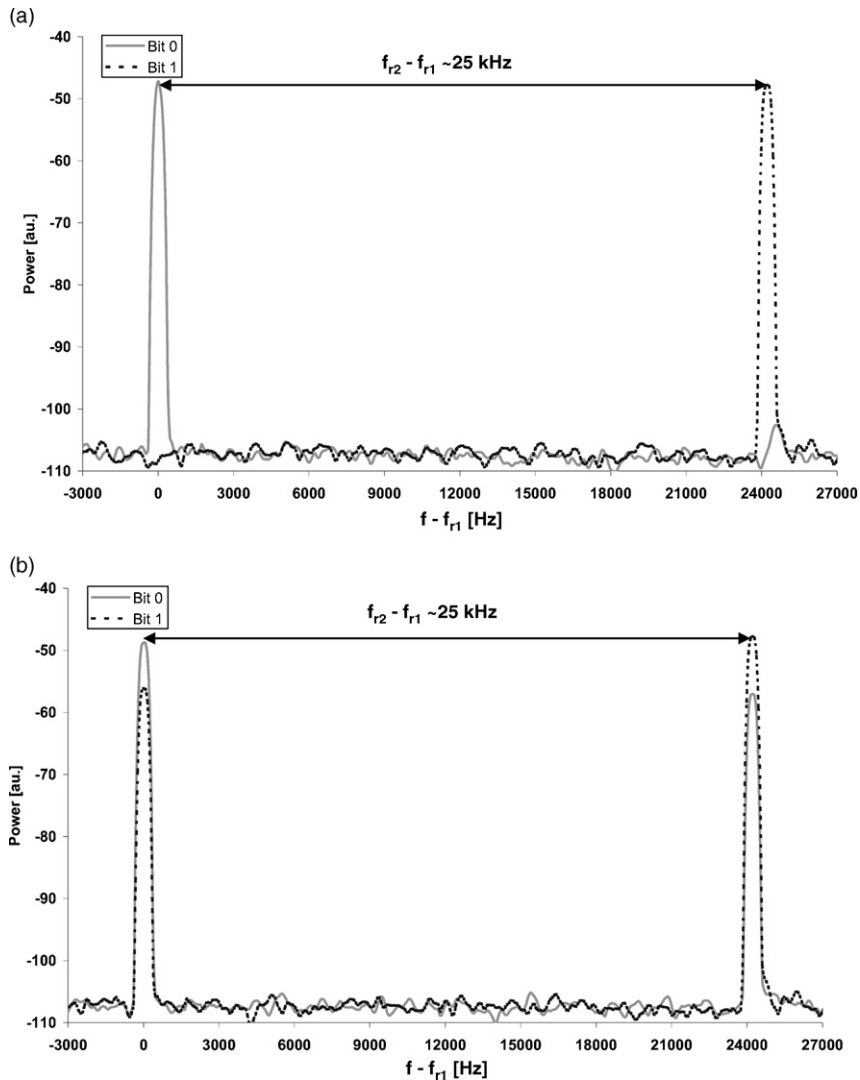

Fig. 9. Schematic representations of received bits 0 and 1: (a) only one eigenmode excited and (b) both modes excited and the information is coded into the relative amplitudes of the resonances. In both cases the bit 0 and bit 1 are represented by solid and dashed lines, respectively.
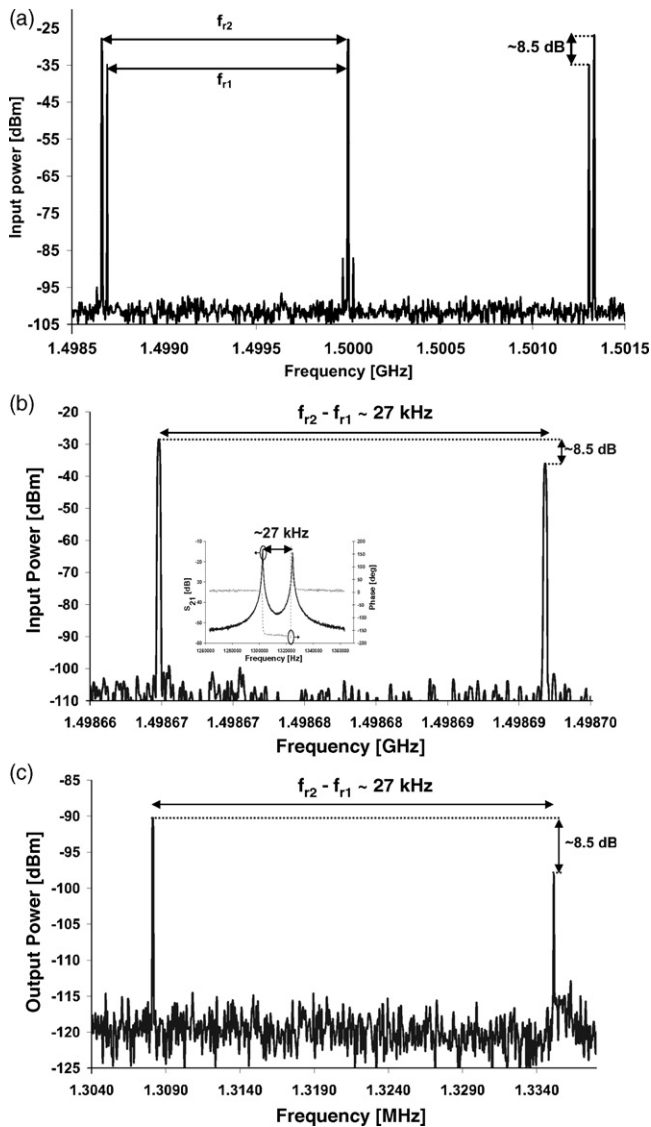
Fig. 10. The spectrum of the signal used in the signal reception measurement of the FSK-receiver. (a) Carrier ($f_c = 1.5$ GHz) and sidebands at the distance $f_{r1} = \pm1.308$ MHz and $f_{r2} = \pm1.335$ MHz from the carrier; (b) detailed view of lower sidebands. (c) The measured signal from the IF-electrode of the resonator indicates that the relative amplitude difference of the input signal at GHz is maintained through the down-conversion of the signal. All the cases represent a situation when bit 0 is transmitted.

corresponding to the eigenmodes of the resonator. This could be done in at least two ways (Fig. 9):

(i) the information is coded so that only one mode of the resonator is excited: lower eigenmode corresponds to the bit 0 and higher eigenmode corresponds to the bit 1 or;

(ii) both modes of the resonator are excited and the information is coded into the relative amplitudes of the resonances: bit 0 is transmitted when the lower resonance is stronger and bit 1 is transmitted when the higher resonance is stronger.

The first approach is straightforward as long as the frequency separation and the Q-factor of the eigenmodes are sufficient to avoid the coupling of the modes. To test the latter approach a

signal having a spectrum shown in Fig. 10(a) and (b) is coupled to the RF-electrode and the output is read from the IF-electrode. The input signal is selected so that the sidebands closer to the carrier are separated from the carrier by $f_{r1} = 1.308$ MHz and the further sidebands by $f_{r2} = 1.335$ MHz. The separations coincide with the first and the second eigenfrequency of the resonator, respectively. In this measurement the amplitudes of the sideband components differ by 8.5 dB. Fig. 10(c) shows the output signal picked from the IF-electrode. It clearly shows that the same relative amplitude difference of the input signal is maintained through the down-conversion of the signal. This indicates that the principal idea of utilising multiresonant micromechanical resonator as an FSK-receiver is a valid one.

4. Discussion and conclusions

The weakness of the down-converted signal can be partially explained by very weak coupling of the RF-signal to the resonator as the characteristic impedance of the resonator is much higher than 50 Ω. With proper impedance matching the performance will be improved as is later shown. Additional explanation comes from Eq. (2) as the force at the resonance frequency is the product of two fairly weak ac-signals a strong LO-signal being absent. However, the situation could be improved by using FM-modulated signal and with the aid of parametric amplification as suggested in [4]. If the carrier frequency component is not needed, the signal can be suppressed carrier AM-signal. In this case the modulation frequency f_m is half the resonance frequency of the MEMS-resonator. The main benefit of this method is the reduced bandwidth at the cost of giving a rather modest output signal strength. On the other hand, if the bandwidth is not an issue, the excitation force can be increased by using aforementioned FM-modulated signal. The approach taken here is very suitable for "wake-up" type radios for wireless sensor networks as the receiver uses essentially zero power due to the absence of a local oscillator.

The utilisation of high Q-factor resonant devices in radio architecture can make the receiver very selective due to the narrow band filtering enabled by the high Q-factor. On the other hand, the high Q-factor leads to rather long excitation and settling times of the resonances, which has a drawback that the achievable data rates will be moderate at best. Some improvement to the data rate can be achieved by coupling additional DETF-periods. Each additional DETF adds a new eigenmode to the system, which can be utilised when transmitting more complex bit series [11].

The accurate model generated gives also the possibility to probe the possibilities of the device. The impedance matching will become feasible once the coupling gaps can be fabricated $d < 100$ nm. Also, the parasitic capacitances originating from the wire bonding pads can be reduced significantly for an actual integrated device. With these modifications to the model, the performance of the device can be seen to improve approximately 50 dB (Fig. 11).

The work done here is yet another demonstration suggesting the feasibility of the concept of a micromechanical radio.
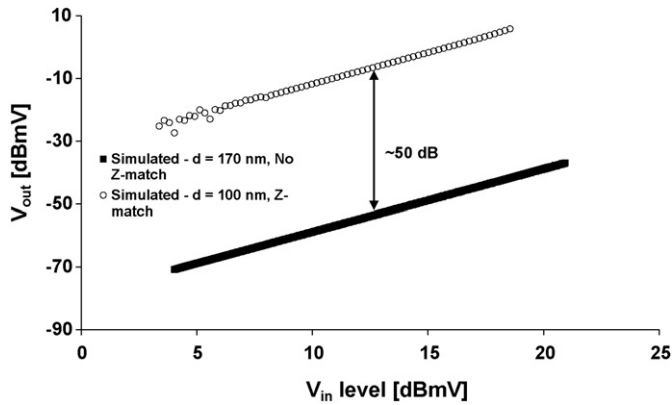
Fig. 11. The impedance match and the reduction of bonding pad capacitances increase the performance of AM-modulated signal down-conversion by almost 50 dB.

Acknowledgements

References

[1] L. Lin, et al., Micro electromechanical fitters for signal processing, *Tech. Digest IEEE MEMS '92, Travemunde, Germany February* 4–7 1992. pp. 226–231.

[2] T. Lee, Design of CMOS Radio-Frequency Integrated Circuits, Cambridge University Press, Cambridge, 1998.

[3] A.-C. Wong, C.T.-C. Nguyen, Micromechanical mixer-filters ("Mixlers"), J. Microelectromech. Syst. 13 (2004) 100–112.

[4] A.T. Alastalo, et al., A micromechanical resonating RF-mixer, in: Proceedings of EUMC2004, Amsterdam, The Netherlands, October 12–14, 2004, pp. 1297–1300.

[5] F. Chen, et al., CMOS-MEMS Resonant RF Mixer-Filters, in: Tech. Digest IEEE MEMS 2005, Miami, USA, January 30–February 3, 2005, pp. 27–30.

[6] B.P. Otis, et al., An ultra-low power MEMS-based two-channel transceiver for wireless sensor networks, in: Proceedings of Symposium on VLSI Circuits, Honolulu, Hawaii USA, June 17–19, 2004, p. 20.

[7] J. Kiihamäki, et al., Fabrication of single crystal silicon resonators with narrow gaps, in: Tech. Digest Transducers '05, Seoul, Korea, June 5–9, 2005, pp. 1354–1357.

[8] Aplac RF Design Tool, AWR-APLAC Corp. [Online] Available: www. aplac.com.

[9] T. Veijola, T. Mattila, Modelling of non-linear micromechanical resonators and their simulation with the harmonic-balance method, Int. J. RF Microw. CAE 11 (2001) 310–321.

[10] S. Maas, Non-linear Microwave and RF-circuits, second ed., Artech House, Norwood, MA, 2003.

[11] A.T. Alastalo, et al., Microelectromechanical delay lines with slow signal propagation, J. Micromech. Microeng. 16 (2006) 1854–1860.

Biographies

M. Koskenvuori received his MSc degree in electrical engineering in 2002 from Helsinki University of Technology (TKK), Finland. Since then he has been working as a research scientist at the TKK pursuing his PhD currently in the laboratory of Micro- and nanosciences. His main research interests are RF-micromechanics and microsystems.

I. Tittonen received his MSc and Dr Tech degrees from the department of technical physics at Helsinki University of Technology (TKK), Finland in 1988 and 1992, respectively. The years 1995–1997 he worked as the Alexander von Humboldt stipendiat at the University of Konstanz, Germany. Since the beginning of the year 2001 Dr Tittonen has been appointed as the professor of physics at TKK. Currently, he is with the laboratory of Micro- and nanosciences. His current research interests are microsystems, nanotechnology and atom optics.